Bull. Mater. Sci., Vol. 40, No. 5, September 2017, pp. 1021–1028
DOI 10.1007/s12034-017-1457-2

Effect of the method for producing Cu–Cr_3C_2 bulk composites on the structure and properties

M A ERYOMINA[1,*], S F LOMAYEVA[1], S N PARANIN[2], S L DEMAKOV[3] and E P YELSUKOV[1]

[1]Physical-Technical Institute, Ural Branch of Russian Academy of Sciences, Izhevsk 426000, Russia
[2]Institute of Electrophysics, Ural Branch of Russian Academy of Sciences, Ekaterinburg 620016, Russia
[3]Ural Federal University named after the first President of Russia B.N. Yeltsin, Ekaterinburg 620002, Russia
*Author for correspondence (mrere@mail.ru)

MS received 20 January 2016; accepted 13 December 2016; published online 30 August 2017

Abstract. Copper–chromium carbide composites containing a carbide phase of 20–30 vol% were obtained with the use of solid- and liquid-phase mechanosyntheses, followed by magnetic pulse compaction (MPC) and spark plasma sintering. The morphology, structural-phase composition, density, hardness and electrical conductivity of the composites were investigated. The structure of composites obtained by MPC represents regions of copper matrix hardened by superfine carbide precipitates surrounded by a layer of chromium carbide. In the composites obtained by spark plasma sintering, the copper matrix hardened by superfine carbide precipitates was divided into areas surrounded by a copper–chromium layer. A composite obtained by the MPC of the powders synthesized using solid-phase mechanosynthesis (MS) (copper, chromium and graphite) had the highest values of Vickers microhardness (4.6 GPa) and Rockwell hardness (HRA 69). The best value of electrical conductivity (36% IACS) was achieved using liquid-phase MS (copper, chromium and xylene) and spark plasma sintering. Liquid-phase MS is the only way to synthesize the powder with a small amount of the carbide phase and without contamination.

Keywords. Mechanosynthesis; nanocomposites; copper; chromium carbide.

1. Introduction

Nanocomposites based on copper reinforced with small amounts of a hardening agent (carbides, oxides, nitrides, borides or phosphides of transition metals) have an optimum combination of good electrical conductivity, thermal conductivity, strength, hardness, damping characteristics and corrosion resistance. Copper nanocomposites have broad potential application as electric contact materials. The nanostructured composites can be prepared in one step, i.e., without preliminary synthesis of the hardening additive. For this purpose, mechanoactivation of metal powders and a solid, liquid or gaseous source of C, O, N, B or P is used [1–8]. The most effective and practically the only way to obtain copper nanocomposites with low amounts of reinforcing components is mechanosynthesis (MS) using a liquid phase (water, liquid hydrocarbons, organic acids, etc.) as a dispersant. However, the effect of such additives on the chemical composition, structural-phase state and properties of the mechanically synthesized composites has rarely been evaluated. However, Lopez *et al* [9] showed that upon preparation of Cu–2 vol% Cr_3C_2 composites by the mechanical activation of powders of copper and chromium carbide with the addition of ethylene glycol; the powders were significantly contaminated with iron, carbon, oxygen and inclusions of iron and chromium oxycarbides, which resulted in a decrease in the ductility and electrical conductivity of the bulk composite. The high hardness of chromium carbide is one of the causes of sample contamination with iron and the formation of oxycarbides is due to the destruction of ethylene glycol molecules.

Previously, we synthesized Cu–30 vol% Cr_3C_2 by two methods: mechanically alloying powders of copper, chromium and graphite in argon and mechanically alloying copper and chromium powders in xylene, which served as a carbon source [10,11]. It has been shown that chromium carbide forms through MS in the presence of graphite. Upon synthesis in xylene, carbide phase formation occurred during subsequent heat treatment of the powders. In this case, grains of the copper matrix and carbide inclusions were smaller even after annealing at 800°C. It is expected that MS with the use of a liquid hydrocarbon would be an effective way to obtain composites with good mechanical properties and a lower carbide phase.

In addition to the choice of powder composite synthesis method, it is important to choose the method of powder compaction. To prepare high-density bulk composites by cold and hot isostatic pressing, severe plastic deformation, magnetic pulse compaction (MPC) and spark plasma sintering (SPS) are the most commonly used [12–15]. The two last methods are the most promising; however, data on the properties of Cu–Cr_3C_2 composites prepared using these methods are not available.

The purpose of this work was to choose optimal methods for producing Cu–Cr_3C_2 composites. To this end, the

structural-phase state and properties (density, hardness and electrical conductivity) of composites produced by solid- and liquid-phase mechanical synthesis methods and compacted by MPC or SPS were evaluated. As a rule, to noticeably improve the mechanical properties of copper products without significantly reducing the electrical conductivity, a hardening phase of 0.5–10 vol% is added to the composite. However, a small amount of the carbide phase makes the study of such composites by X-ray diffraction and microscopy difficult. In this paper, the basic research was carried out on model alloys containing chromium and carbon corresponding to 30 vol% Cr_3C_2.

2. Materials and methods

To prepare the samples, 72.7 wt% copper (99.72 wt%, average particle size 17 μm), 21.0 wt% chromium (99.92 wt%, 17 μm) and 3.3 wt% graphite (99.99 wt%, ∼1000 μm) powders and ∼20 cm^3 of xylene as a carbon source were used. This composition corresponded to the following composition in atomic percents: $Cu_{63.9}Cr_{21.7}C_{14.4}$. The chosen proportion of the components corresponded to the volume concentration of chromium carbide Cr_3C_2 of 30%. MS was performed in a planetary ball mill (Fritsch P-7, Germany) with forced air cooling. The containers (volume of 45 cm^3) and the balls (20 pieces, 8 mm in diameter) were made of steel (1 wt% C, 1.5 wt% Cr). The treatment time was 24 h and the weight of the loaded powder mixture was 10 g. The solid-phase milling of the Cu–Cr–graphite powders was performed under low excessive pressure of a purified argon atmosphere. The liquid-phase milling of Cu–Cr powders was performed in the containers filled with xylene. The samples obtained through solid- and liquid-phase syntheses are denoted as P1 and P2, respectively (table 1). Sample P3 with 5 vol% Cr_3C_2 was obtained by MS in xylene for 48 h. The powders were annealed in argon at 600–800°C (1 h) and the annealed powders were designated as P1-600, P1-800, P2-600 and P2-800. Annealing of the powders in argon atmosphere allows us to estimate the sintering temperatures.

MPC [16–18] and SPS [19] were selected as methods of compacting. The amplitude of the pulse wave of compression of MPC was 1.5 GPa with a pulse duration of 300 ms. Before compaction, the samples were degassed at heating to a temperature of 500°C under vacuum (5–10 Pa) for 240 min and then pressed between steel strips coated with a layer of graphite at a temperature of 500°C. To prevent cracking, the samples were cooled to 400°C and then to room temperature for 120 min. Disks 15 mm in diameter with a thickness of 1–2 mm were obtained. The composite obtained from P1 is designated in table 1 as M1, from P2 as M2 and that from P3 as M3.

SPS was performed using an HP D 25 (FCT Systeme GmbH, Germany) system with a pulse duration of 5 ms, a constant voltage of 4.5 V and a current of 810 A. The powders were charged between two graphite electrodes in cylindrical graphite crucibles with inner and outer diameters of 20 and 60 mm, respectively. Sintering was carried out in a vacuum of 10^{-1} Pa at a pressure of 80 MPa. The powders were degassed, then heated at 100°C min^{-1} to a temperature of 700°C and then held for 30 min, after which the furnace was cooled to room temperature. The diameter of the obtained disks was 20 mm and the thickness was 1–2 mm. In table 1, S1 and S2 denote the composites obtained from powders P1 and P2, respectively.

X-ray photoelectron spectroscopy (XPS) was used to determine the surface composition of the powder particles.

Table 1. Characteristics of experimental samples: volume fraction of carbide, copper lattice parameter (a_{Cu}), grain size ($\langle L\rangle_{Cu}$), copper lattice microstrain level (ε), density (ρ), microhardness (HV), HRA hardness and electrical conductivity of the samples.

Sample	Preparation	Volume fraction of carbide (%)	a_{Cu} (nm)	$\langle L\rangle_{Cu}$ (nm)	ε (%)	ρ (g cm^{-3})	ρ (%)	HV (GPa)	HRA	% IACS
P1	MS (graphite)	30(2)	0.3626(1)	3(1)	0.10(2)	—	—	—	—	—
P1-600	MS (graphite), annealing at 600°C	30(2)	0.3620(1)	7(2)	0.02(1)	—	—	—	—	—
P1-800	MS (graphite), annealing at 800°C	30(2)	0.3618(1)	48(5)	0.04(1)	—	—	—	—	—
P2	MS (xylene)		0.3622(1)	4(1)	0.05(2)	—	—	—	—	—
P2-600	MS (xylene), annealing at 600°C		0.3619(1)	7(1)	0.03(1)	—	—	—	—	—
P2-800	MS (xylene), annealing at 800°C	21(2)	0.3618(1)	31(4)	0.02(1)	—	—	—	—	—
P3	MS (xylene)		0.3617(1)	9(3)	0.04(2)	—	—	1.2(1)	—	—
M1	P1, MPC	30(2)	0.3617(1)	11(8)	0.05(3)	7.79(5)	96	4.6(4)	69(2)	19(2)
M2	P2, MPC		0.3618(1)	9(2)	0.02(2)	7.90(5)	96	3.8(4)	—	15(2)
S1	P1, SPS	22(2)	0.3618(1)	22(5)	0.06(1)	7.50(5)	88	4.0(3)	58(2)	26(2)
S2	P2, SPS	20(2)	0.3618(1)	21(4)	0.07(1)	7.98(5)	98	3.8(2)	63(1)	36(2)
M3	P3, MPC		0.3616(1)	13(3)	0.01(2)	7.67(5)	93	2.3(2)	—	30(2)

The XPS spectra were obtained on an ES-2401 spectrometer (EZAN, Russia). The vacuum in the analyser chamber was approximately 10^{-7} Pa. The calibration of the spectra was carried out under Au $4f_{7/2}$ (84.0 eV). The value of the binding energy (E_b) of the electron line, C1s, in the alkyl group was taken to be 285.0 eV. The accuracy of the position of the line was ±0.2 eV. The relative accuracy of the quantitative analysis was ±10%. Analysis of the XPS spectra was performed in accordance with Briggs and Seah [20], Beamson and Briggs [21] and Povstugar *et al* [22].

X-ray diffraction analysis was carried out using two X-ray diffractometers: a DRON-3 Min X-ray diffractometer with CuKα radiation at 2θ from 20 to 110°C and the software package MIS&S [23] and a MiniFlex (Rigaku) X-ray

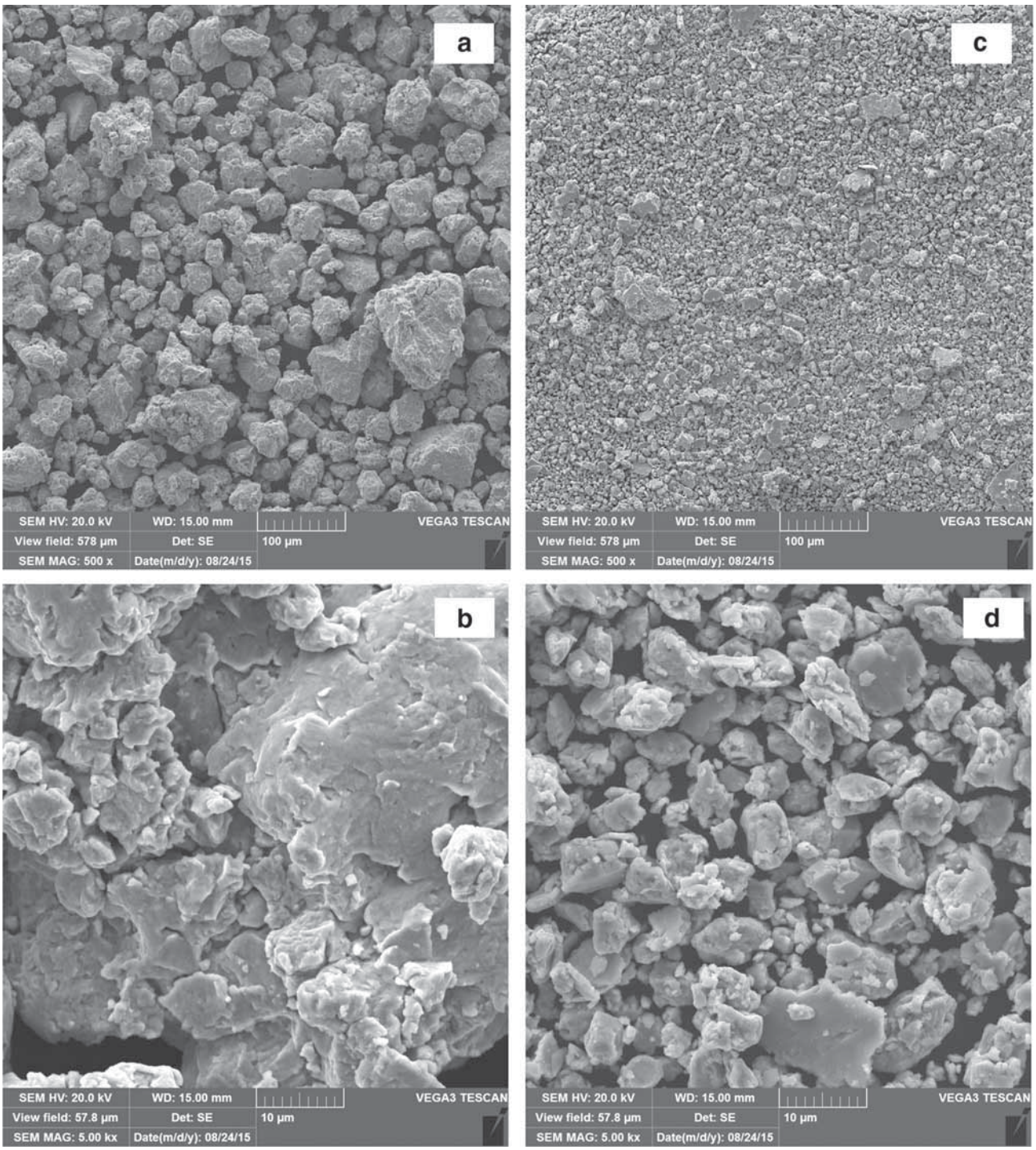

Figure 1. SEM images of the (**a**, **b**) P1 and (**c**, **d**) P2 powders.

diffractometer with Co Kα radiation at 2θ from 20 to 130°C and the software package PDXL. A quantitative analysis was carried out using Rietveld refinement [23]. The grain size of the copper was evaluated using the diameter of the regions of coherent scattering as determined by the Warren–Averbuch method using a one-line profile in accordance with Dorofeev *et al* [24]. All composites prior to the study of the structural-phase state and properties were mechanically polished.

The morphology, microstructure and distribution of the main components were investigated using two scanning electron microscopes (SEMs): a JEOL JSM-6490LV SEM with a system for microscopic X-ray analysis (INCA Energy 350, Oxford Instruments) and a VEGA 3 LMH (TESCAN) SEM with a system for X-ray energy dispersive microanalysis (INCA Energy 250/X-max 20, Oxford Instruments). Both systems were used at accelerating voltages of 20 kV with preliminary chemical etching of the polished composites.

To measure the microhardness, HV, of the composites, the device PMT-3 was used with a load of 0.49N for 10 s. Each sample was measured ten times. Hardness measurements were carried out by the Rockwell method in HRA units. In this case, each sample was measured five times. All the samples were polished. Mean values and standard deviations were calculated. The density of the composites was evaluated by hydrostatic weighing. The electrical conductivity was measured at room temperature by the standard four-probe method using V1–13 as the current source and R3009 as the bridge.

3. Results and discussion

Figure 1 shows images of the obtained powders. The powders are agglomerated and the sizes of the agglomerates of the P1 powder particles obtained by MS with graphite are 20−100 μm (figure 1a and b). According to X-ray diffraction, P1 is a nanocrystalline solid solution of chromium in copper with a grain size of approximately 3 nm. The weak halo between 2θ of 35−55° corresponds to a phase of nanodispersed Cr_3C_2 (figure 2a, curve 1) [11]. The grain size of the copper matrix (table 1) remains virtually unchanged after annealing at 600°C (sample P1-600) and increases markedly after annealing at 800°C (sample P1-800). The grain size of the P1-600 powder is close to 7 nm and the grain size of the P1-800 powder is close to 48 nm. Therefore, the sintering temperature should be below 800°C. The volume fraction of Cr_3C_2 in the samples P1-600 and P1-800, evaluated by quantitative X-ray analysis, was close to 30%.

Use of a liquid organic medium in MS reduced the sizes of the agglomerates of the P2 powder particles to 5−10 μm (figure 1c and d). The X-ray diffraction patterns show only a nanocrystalline solid solution of chromium in copper with a grain size of 4 nm and nanocrystalline chromium (figure 2b and table 1). The grain size of the copper matrix is close to 7 nm (P2-600) after annealing at 600°C and it increased up to 31 nm (P2-800) after annealing at 800°C. Despite the fact that according to the Auger analysis [11], the amount of carbon on the particles obtained in xylene was three times greater than in the case of graphite, carbide formation in the MS process did not occur. After annealing at 600°C (sample P2-600), the nanocrystalline chromium lines disappear and broad peaks with low intensities, which can be attributed to

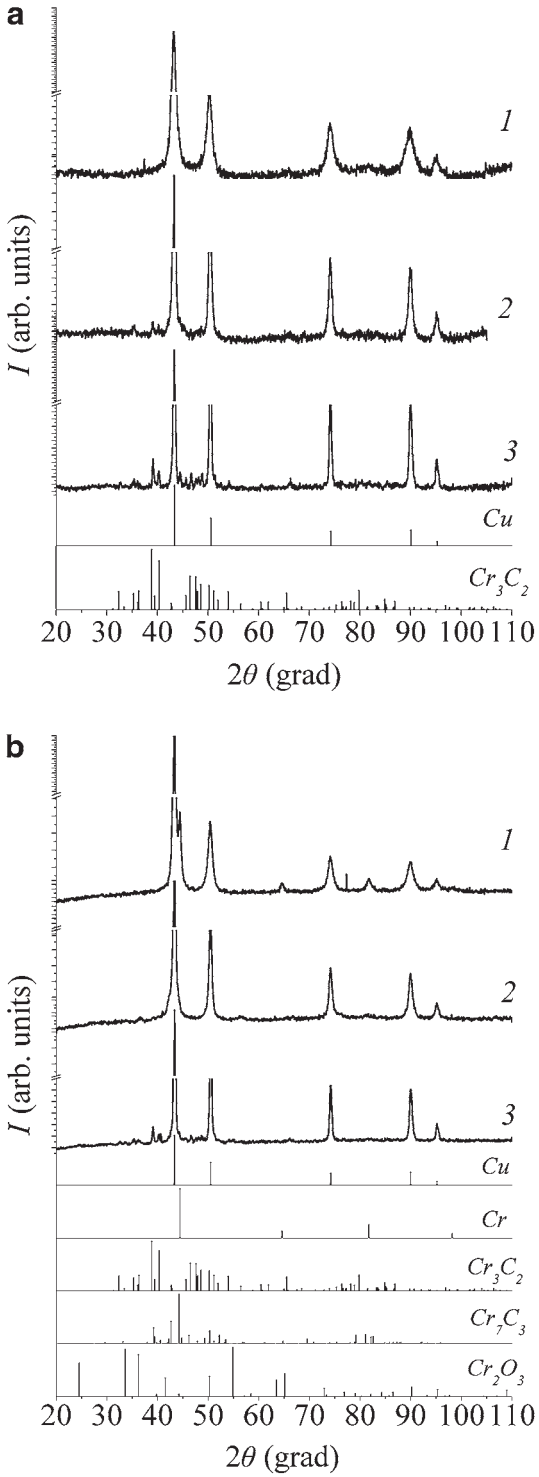

Figure 2. Powder XRD patterns of (**a**1) P1, (**a**2) P1-600, (**a**3) P1-800, (**b**1) P2, (**b**2) P2-600 and (**b**3) P2-800.

highly dispersed carbide, Cr_3C_2, appear in the diffraction pattern. After annealing at 800°C (sample P2-800), the formation of approximately 21 vol% of chromium carbides, Cr_3C_2 and Cr_7C_3 and 3 vol% of an oxide, Cr_2O_3, is observed. The carbide Cr_7C_3 most likely formed due to the partial oxidation of carbon. Thus, in the powders obtained by MS in xylene, the formation of fine chromium carbides occurs but only after further annealing. It should be noted that according to the results of the energy dispersive X-ray analysis of MS with the use of graphite, slight contamination of the powder by the grinding media (1.5 at% iron) occurred. With MS in xylene, iron contamination was absent.

The presence of oxides in the powders after annealing may be related to the composition of the surface and also to the higher specific surface area of the powders obtained in xylene. The composition of the surface was investigated by XPS (figure 3). In the C1s spectra, the line with $E_b = 285.0$ eV corresponds to the hydrocarbon in the group $(-CH_2-CH_2-)_n$ and the line with $E_b > 286.0$ eV corresponds to the oxidized carbon. In the O1s spectrum, the line with $E_b \approx 530$ eV corresponds to the metal oxides, the line with $E_b \approx 531.6$ eV denotes hydroxides and the line with $E_b > 533$ eV corresponds the oxygen atoms in the composition of the adsorbed water. In the Cu2p spectrum, the line with $E_b \approx 933$ eV may correspond to both Cu and Cu_2O, whereas the line with $E_b \approx 935.3$ eV corresponds to $Cu(OH)_2$. The Cr2p spectrum is represented by the wide line with a maximum $E_b \approx 577$ eV, characteristic of chromium compounds in the state of Cr^{3+}. Based on the line width, the contribution to the spectrum is given by oxides and hydroxides of chromium. The analysis showed that significantly more oxidized carbon, adsorbed water and metal hydroxides exist on the surface of the sample obtained by MS with the use of graphite, P1. Despite this, reduction of the metal from the oxide was faster in P1 than in P2 owing to the lower specific surface area. Compaction conditions were selected based on the analysis of the initial and annealed powders.

Curve 1 of figure 4 shows the X-ray diffraction pattern of the M1 composite, which was compacted by MPC from the P1 powder obtained with the use of graphite. During MPC, the copper matrix grains grew to ∼10 nm and the microstrain decreased to 0.02–0.05%. Carbide lines in the X-ray diffraction patterns had very low intensities and broadened considerably, which points to the nanocrystalline state of the carbide phase.

Figure 5a presents low- and high-magnification electronic images of the surface of the M1 composite. In the images, borders of the initial agglomerates of the particles are not observed. Chromium carbide is present in the form of rounded inclusions of approximately 100 nm in size, with some inclusions of 1−3 μm in size (in the electronic images, carbide is shown as dark areas). The higher magnification image shows that the small carbide inclusions form nets, with an average cell size of up to 5 μm, which are evenly distributed over the volume of the composite. The atomic ratio of the concentrations of Cu:Cr in the copper matrix is 74:26, which is close to the initial value of 75:25. The sizes of the cells are close to the primary particle size (figure 1b). Thus, in this case, compacting has no significant effect on the morphology formed during mechanosynthesis. The single light area on the electronic image in figure 1a is an area rich in copper (Cu:Cr = 93:7). Its presence is due to the entry of the particles from 'dead' zones of the grinding container into the composite.

The microhardness of composite M1 is 4.6 GPa, its Rockwell hardness is 69(2) HRA and its electrical conductivity is 19% IACS.

Curve 2 of figure 4 shows the X-ray diffraction pattern of the M2 composite compacted by MPC from powder P2 obtained using xylene. In addition to nanocrystalline copper with a grain size of 10 nm, nanocrystalline carbides (Cr_3C_2 and Cr_7C_3) and an oxide (Cr_2O_3, ∼3 vol%) are also observed in the annealed powder (table 1). Because the lines of the carbides are broadened and there are sets of lines from different carbides, the exact proportions of Cr_3C_2 and Cr_7C_3 cannot be determined.

In the electronic images of the M2 composite (figure 5b), large areas from 1 to 50 μm with the atomic ratio of Cu:Cr = 74:26 surrounded by carbide layers with thicknesses of 5 μm

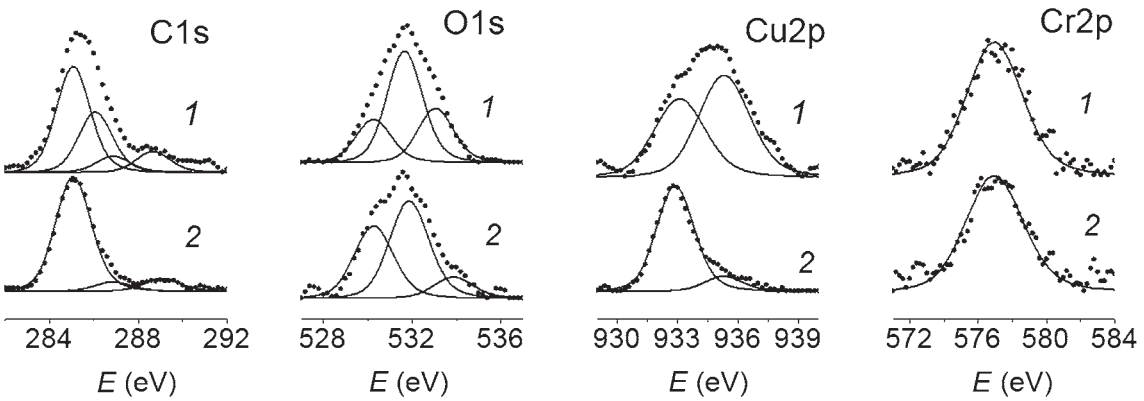

Figure 3. XPS spectra of the (1) P1 and (2) P2 powders.

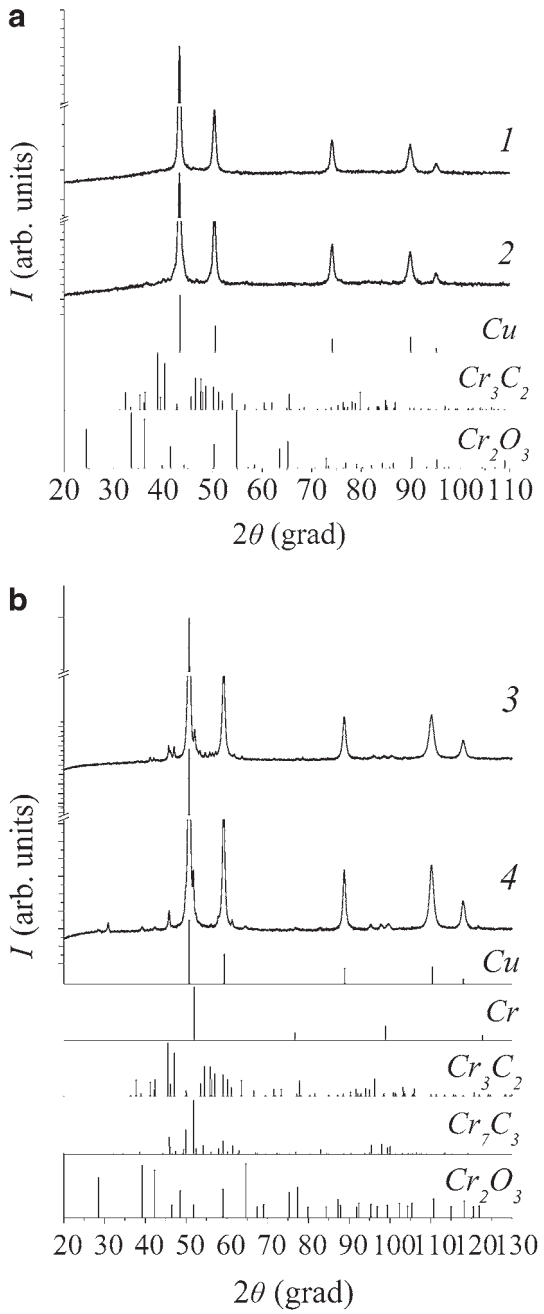

Figure 4. XRD patterns of the composites. 1, 2: M1, M2 (CuKα), respectively and 3, 4: S1, S2 (Co Kα), respectively.

were observed. The sizes of these areas do not coincide with the size of the agglomerates or the particle size of the initial powder. In this case, therefore, the morphology of the composite is formed during compacting. Within the regions, there are rare carbide inclusions ranging from 100 nm to 1 μm. However, the microhardness of the areas free of visible carbide inclusions is high (3.8 GPa), which indicates the presence of reinforcing carbide inclusions less than 100 nm in size. The electrical conductivity of M2 is 15% IACS. The densities of the M1 and M2 composites are the same: 96% of the theoretical value.

Thus, regardless of the powder's synthesis method, the structure of MPC composites represents regions of copper matrix hardened by superfine carbide precipitates surrounded by a layer of chromium carbide. The use of graphite in the synthesis of the powder allows us to obtain a more uniform distribution of chromium carbide over the volume of the composite, thus increasing the composite microhardness somewhat.

Curves 3 and 4 of figure 4 show X-ray diffraction patterns of composites S1 and S2, prepared by SPS. The phase composition of S1 is more complicated than that of the annealed powder P1 (table 1). In addition to copper with a grain size of ∼20 nm, approximately 3 vol% Cr, 4 vol% Cr_2O_3 and 22 vol% Cr_3C_2 are present in the phase composition of the composite. Grey areas with the atomic ratio of Cu:Cr = 73:27 and with sizes corresponding to the particle size of the starting P1 powder surrounded by light layers with a thickness of 1−10 μm are seen in the electronic images (figure 5c). Copper dominates in the composition of the light layers (Cu:Cr = 97:3). Chromium carbide in the form of dispersed inclusions with an average size of approximately 70 nm is uniformly distributed in the grey areas. The sizes of very rare large inclusions are no greater than 1 μm. The density of the S1 composite is 88%, the microhardness is 4.0 GPa, the Rockwell hardness is 63 HRA and the electrical conductivity is 26% IACS.

It is obvious that during compaction by SPS, decarbonization of the surface layer of the powder P1 particles, the partial oxidation of chromium and Cr_3C_2 that forms in the MS process and the melting of the lowest-melting-temperature component (copper) occur under the action of the spark energy. The particles are effectively welded together; molten copper fills the spaces between the particles. Free chromium partly remains in the 'welded' areas as part of a solid solution; it is also present in the form of fine oxide precipitates. The presence of copper layers increases the electrical conductivity of S1 as compared to the M1 composite. However, M1 has a higher density. This is likely due to the large amount of water vapour on the surface of P1 (figure 3), which, during the prolonged evacuation (4 h) before MPC, is completely removed, which does not occur in short-term exposure before SPS.

The phase composition of the S2 composite, unlike S1, does not contain free chromium and Cr_3C_2. This composite was formed of 20 vol% Cr_7C_3, approximately 3 vol% Cr_2O_3 and a solid solution based on copper with a grain size of approximately 20 nm. As indicated previously, the formation of the carbide phase in composites synthesized in xylene occurs only when heat is treated. The formation of carbide with lower carbon content is related to the fact that the particle size of the P2 powder is much less than that of P1 and that decarbonization affects almost the entire volume of the compacted powder particles. The microstructure of the composite S2 (figure 5d) is analogous to the microstructure of S1, but the sizes of the 'grey' areas surrounding the grains is much smaller (5 μm), which corresponds to the particle size of the starting powder.

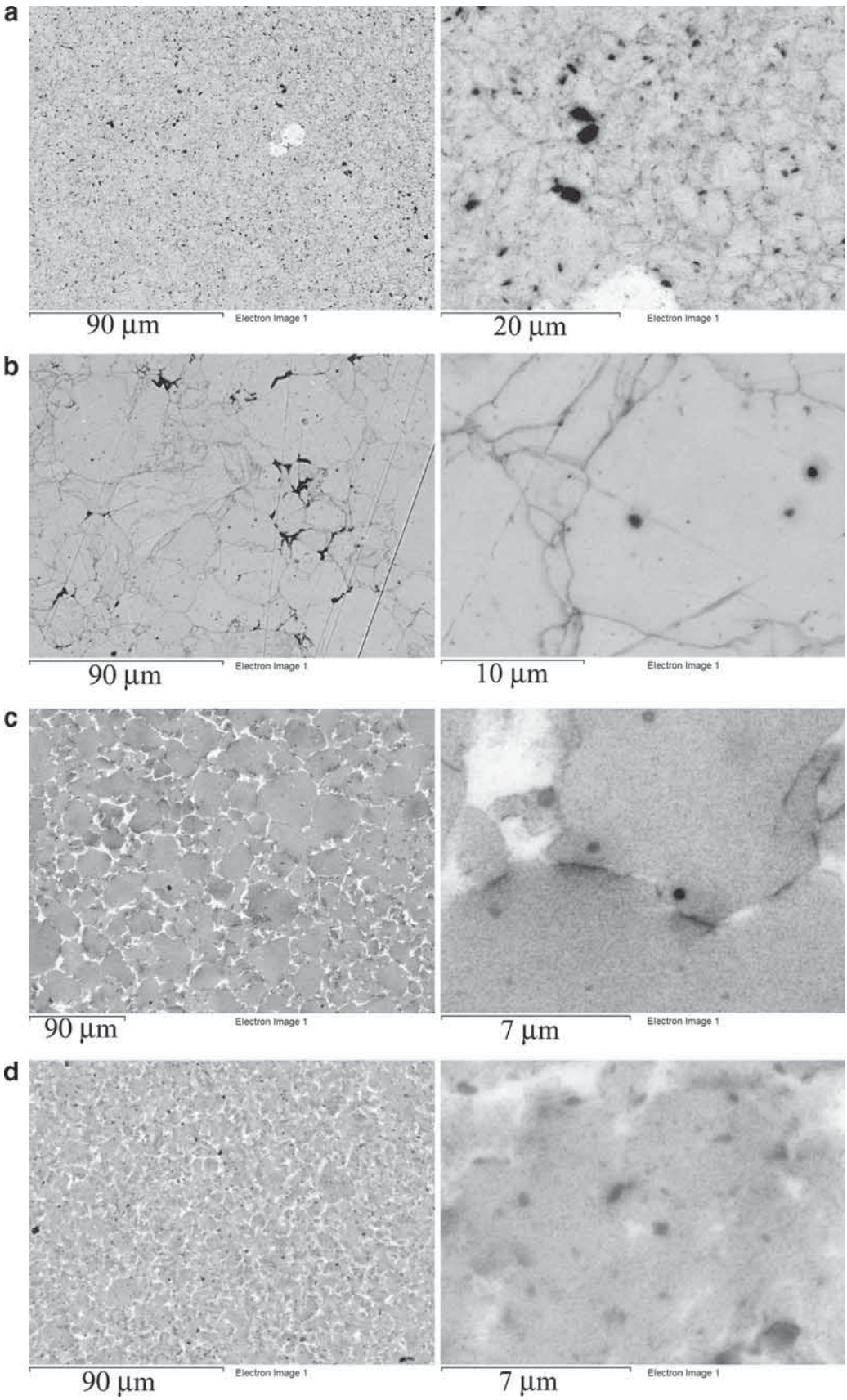

Figure 5. SEM images of the (**a**) M1, (**b**) M2, (**c**) S1 and (**d**) S2 composites.

The microhardness of S2 (3.8 GPa) is close to that of S1, but the density of S2 (98%) and its Rockwell hardness (63 HRA) are higher. The electrical conductivity (36% IACS) is much greater than that obtained for all other composites (see table 1) due to the presence of substantially pure copper layers in the microstructure of the composite and its high density.

Obviously, the SPS method is the most effective one for producing composites with the highest electrical conductivity. However, to attain high values of microhardness, it is more effective to apply the MPC method.

Since decarbonization of the powders mechanosynthesized in xylene proceeded more vigorously during SPS, the MPC method was used to obtain the composite M3 containing 5 vol% Cr_3C_2. According to the X-ray diffraction data, the obtained M3 and P3 are in the single-phase state comprising nanocrystalline copper with a grain size of 13 nm (table 1). Therefore, the properties of the composite obtained were compared to the properties of nanocrystalline copper produced by equal-channel angular extrusion (16 passes). The microhardness of M3 (2.3 GPa) was two times higher than that of nanocrystalline copper and the electrical conductivity (30% IACS) was three times lower.

4. Conclusion

Bulk Cu–Cr_3C_2 (Cr_7C_3) composites with a carbide content of 20–30 vol% were prepared by MPC and SPS of powders mechanically synthesized in an inert gas (argon) using graphite and in a liquid hydrocarbon (xylene). X-ray diffraction, electron microscopy and measurements of hardness, density and electrical conductivity were used to investigate the effect of synthesis method and the method of their consolidation on the structure and properties of the resulting composites.

It has been shown that the composites had a nanostructured copper matrix with inclusions of fine carbides ranging in size from 70 nm to 3 μm and that the matrix is divided into areas surrounded by a carbide layer at MPC or by a copper layer at spark plasma sintering. The morphology of the composite influenced its properties. The composite obtained by MPC of powders synthesized with the use of graphite had the highest microhardness of 4.6 GPa, a Rockwell hardness of 69 HRA and an electrical conductivity of 19% IACS. The highest electrical conductivity of 36% IACS, a microhardness of 3.8 GPa and a Rockwell hardness of 63 HRA, was achieved by using mechanical synthesis in xylene and spark plasma sintering.

Acknowledgements

This work was supported by the Government of the Russian Federation (Federal Agency for Scientific Organizations) under the themes of the state task, no. 0389-2014-0002 and no. 0428-2014-0002 and by the Program of UD RAS, Project reg. no. AAAA-A17-117040610324-3.

References

[1] Mahbub Ullah, Md Eaqub Ali and Sharifah Bee Abd Hamid, 2014 *Rev. Adv. Mater. Sci.* **37** 1
[2] Yazovskikh K A and Lomayeva S F 2014 *J. Alloys Compd.* **586** 565
[3] Lomayeva S F, Yazovskikh K A, Maratkanova A N, Syugaev A V, Timoshenkova O R, Kaygorodov A S *et al* 2013 *Inorg. Appl. Res.* **4** 138
[4] Lomayeva S F, Syugaev A V, Eremina M A, Ul'yanov A L, Yurovskikh A S, Zayats S V *et al* 2014 *Prot. Met. Phys. Chem. Surf.* **50** 352
[5] Yazovskikh K A, Lomayeva S F and Syugaev A V 2014 *Acta Phys. Pol. A* **126** 947
[6] Eryomina M A, Lomayeva S F, Yelsukov E P, Ul'yanov A L and Chulkina A A 2014 *Met. Mater. Int.* **20** 1123
[7] Long B D, Othman R, Zuhailawati H and Umemoto M 2014 *Adv. Mater. Sci. Eng.* **2014** 1
[8] Kung Ch, Liao T-T, Tseng K-H, Chen K-Y and Chuang M-Sh 2009 *Can. Soc. Mech. Eng.* **33** 361
[9] Lopez M, Camurri C, Vergara V and Jimenez J A 2005 *Rev. Metal. (Madrid, Spain)* **41** 308
[10] Eryomina M A, Lomayeva S F, Yelsukov E P, Bodrova L E, Goida E Y and Pastukhov E A 2013 *Khimicheskaia Fizika i Mezoskopiia* **15** 262
[11] Eremina M A, Lomayeva S F and Elsukov E P 2013 *Phys. Met. Metallogr.* **114** 928
[12] Upadhyaya G S 2002 *Powder metallurgy technology* (Great Abington, England: Cambridge International Science Publishing)
[13] Long B D, Umemoto M, Todaka Y, Othman R and Zuhailawati H 2011 *Mater. Sci. Eng. A* **528** 1750
[14] Lee G H, Rhee C K, Lee M K, Kim W W and Ivanov V V 2004 *Mater. Sci. Eng. A* **375** 604
[15] Zhang Zh-H, Wang F-Ch, Wang L and Li Sh-K 2008 *Mater. Sci. Eng. A* **476** 201
[16] Mironov V 1994 *Magnetic pulse pressing of powders and shaping of powder products Proceed Intern Conf PM-94 'Sintering consolidation'*, Paris, France
[17] Olevsky E A, Bokov A A, Boltachev G S, Volkov N B, Zayats S V, Ilyina A M *et al* 2013 *Acta Mech.* **224** 3177
[18] Ivanov V, Kotov Y A and Samatov O H 1995 *Nanostruct. Mater.* **6** 287
[19] Zhang Z N, Wang F C, Lee S K, Liu Y, Cheng J W and Liang Y 2009 *Mater. Sci. Eng. A* **523** 134
[20] Briggs D and Seah M P 1990 *Practical surface analysis* Vol 1 (Chichester, UK: Wiley)
[21] Beamson G and Briggs D 1992 *High resolution XPS of organic polymers: The Scienta ESCA300 Database* (New York: John Wiley & Sons)
[22] Povstugar V I, Shakov A A, Mikhailova S S, Voronina E V and Elsukov E P 1998 *J. Anal. Chem.* **53** 697
[23] Shelekhov E V and Sviridova T A 2000 *Mater. Sci. Heat. Treat.* **42** 309
[24] Dorofeev G A, Povstugar I V, Protasov A V, Elsukov E P and Streletskii A N 2012 *Colloid. J.* **74** 675